




Article

Carboxymethyl Cellulose/Copper Oxide–Titanium Oxide Based Nanocatalyst Beads for the Reduction of Organic and Inorganic Pollutants

Esraa M. Bakhsh ¹, Sher Bahadar Khan ^{1,*}, Nujud Maslamani ², Ekram Y. Danish ¹, Kalsoom Akhtar ¹ and Abdullah M. Asiri ^{1,3}

¹ Chemistry Department, Faculty of Science, King Abdulaziz University, P.O. Box 80203, Jeddah 21589, Saudi Arabia

² Chemistry Department, College of Science, Imam Abdulrahman Bin Faisal University, P.O. Box 76971, Dammam 31441, Saudi Arabia

³ Center of Excellence for Advanced Materials Research, King Abdulaziz University, P.O. Box 80203, Jeddah 21589, Saudi Arabia

* Correspondence: sbhkhan@kau.edu.sa

Abstract: In this work, we have developed novel beads based on carboxymethyl cellulose (CMC) encapsulated copper oxide-titanium oxide (CuO-TiO₂) nanocomposite (CMC/CuO-TiO₂) via Al⁺³ cross-linking agent. The developed CMC/CuO-TiO₂ beads were applied as a promising catalyst for the catalytic reduction of organic and inorganic contaminants; nitrophenols (NP), methyl orange (MO), eosin yellow (EY) and potassium hexacyanoferrate (K₃[Fe(CN)₆]) in the presence of reducing agent (NaBH₄). CMC/CuO-TiO₂ nanocatalyst beads exhibited excellent catalytic activity in the reduction of all selected pollutants (4-NP, 2-NP, 2,6-DNP, MO, EY and K₃[Fe(CN)₆]). Further, the catalytic activity of beads was optimized toward 4-nitrophenol with varying its concentrations and testing different concentrations of NaBH₄. Beads stability, reusability, and loss in catalytic activity were investigated using the recyclability method, in which the CMC/CuO-TiO₂ nanocomposite beads were tested several times for the reduction of 4-NP. As a result, the designed CMC/CuO-TiO₂ nanocomposite beads are strong, stable, and their catalytic activity has been proven.

Keywords: catalytic reduction; carboxymethyl cellulose; nanocatalyst; catalytic reduction; organic and inorganic pollutants



Citation: Bakhsh, E.M.; Khan, S.B.; Maslamani, N.; Danish, E.Y.; Akhtar, K.; Asiri, A.M. Carboxymethyl Cellulose/Copper Oxide–Titanium Oxide Based Nanocatalyst Beads for the Reduction of Organic and Inorganic Pollutants. *Polymers* **2023**, *15*, 1502. <https://doi.org/10.3390/polym15061502>

Academic Editor: Mohammad Afsar Uddin

Received: 30 December 2022

Revised: 3 March 2023

Accepted: 8 March 2023

Published: 17 March 2023



Copyright: © 2023 by the authors. Licensee MDPI, Basel, Switzerland. This article is an open access article distributed under the terms and conditions of the Creative Commons Attribution (CC BY) license (<https://creativecommons.org/licenses/by/4.0/>).

1. Introduction

Large quantities of organic and inorganic contaminants released to the ecosystem through wastewater stream due to different human activities (e.g., industrial waste, textile, agrochemical and pharmaceutical). These organic and inorganic pollutants, such as dyes, nitrophenols, and potassium hexacyanoferrate are naturally unmanageable, highly toxic, hazardous in nature, carcinogenic, mutagenic, and limited biodegradable. They are also seen as being harmful and dangerous to living things [1–5].

As a result, the techniques for removing these types of pollutants have significant drawbacks, such as low elimination rates, high cost and complexity, and slow removal efficiency, which limit their uses. Many efforts have been devoted to remove toxic contaminants from water bodies, but some of the established methods are not useful enough to complete the removal of toxic pollutants, besides long time consumption and their high cost. The demand for pollution management around the world is to develop new cost-effective, environmentally friendly, simple, and new manageable processes to remove the toxic contaminants or convert into the toxins into useful compounds. The rising advancement of usage of green chemistry in pollution management is due to the fact that environmentally friendly processes have a long history of being both environmentally and

economically beneficial [6–8]. Recently, huge efforts have been made to develop methods based on catalytic reduction/degradation/transformation of these toxic contaminants to less toxic form and useful compounds which is a good way to deal with wastewater contaminants. Catalytic reduction is one strategy that requires less time to remove the toxic pollutants, which is easy, fast and involves a very low quantity of solvent compared to other techniques. According to literature, various catalysts have been prepared from an efficient, stable, and selective material to be an efficient for the removal toxic organic and inorganic contaminants from wastewater.

Copper oxide nanocatalyst can achieve good selectivity without any extra additives for reducing nitrophenols and dyes. Due to its unique characteristics, such as a high surface-to-volume ratio and higher activity compared to those of the bulk materials [9–11]. Titanium dioxide (TiO_2) is also frequently used as a nanocatalyst or substrate for immobilizing metal nanomaterial because of its favorable qualities of non-toxicity, stability, and hydroxyl-rich surface [12]. In particular, copper oxide (p-type) and titanium oxide (n-type) are an important class of semiconductor for efficient dye degradation processes and the reduction of nitrophenols. Thus, a nanocatalyst based on the combination of TiO_2 and CuO have been developed for the reduction of nitrophenol and dyes due to their great advantages of adjustable oxidation states, low cost, as well as thermal and chemical stability [13–18]. Unfortunately, the powder nanocatalyst of metal oxides encountered issues like aggregation, difficulties in separation and reuse of these materials [14,19–23].

Polymer-based metal oxide nanocomposite holds great promise as a viable approach to overcome the aforementioned challenges of metal oxide nanoparticles. According to recent studies, different polymer-based nanocomposites have been fabricated by various ways, either by coating or hosting the fine nanomaterial onto the polymer matrix of larger size. Polymeric host materials are an attractive route to control the pore space and surface of the nanomaterials as well as their excellent properties, which could improve the mechanical strength for long-term use. Several polymers, including cellulose or carboxymethyl cellulose [13,24–28], chitosan, agarose, clay, alginate and so on [21,29–36], are used. Among them, CMC has been proven to be an appropriate polymer host for various metal oxide nanocomposites.

In the current study, an efficient nanocatalyst beads were developed based on incorporating the nanocomposite CuO-TiO_2 onto the CMC as a host polymer by the help of cross-linking agent AlCl_3 . CMC/ CuO-TiO_2 beads were characterized by SEM, XRD and EDS. The synthesized CMC/ CuO-TiO_2 beads were evaluated as catalyst for the reduction of selected organic and inorganic pollutants.

2. Experimental

2.1. Chemicals and Reagents

Titanium (VI) oxide (TiO_2) of particle size < 100 nm and purity of $>97\%$ has been provided by Sigma Aldrich. Copper (II) nitrate ($\text{Cu}(\text{NO}_3)_2$), nitrophenols including 4-nitrophenol (4-NP), 2-nitrophenol (2-NP) and 2,6-dinitrophenol (2,6-DNP), organic dyes involving methyl orange (MO) and eosin yellow (EY), potassium hexacyanoferrate $\text{K}_3[\text{Fe}(\text{CN})_6]$, sodium borohydride (NaBH_4), and carboxymethyl cellulose (CMC) were all purchased from Sigma-Aldrich. Distilled water was used in all experiments.

2.2. Synthesis of CuO-TiO_2 Nanoparticles

CuO-TiO_2 nanoparticles were prepared by dissolving cupric nitrate in distilled water (1:1 weight) and stirring thoroughly to completely dissolve the cupric nitrate. Then, the TiO_2 was added to cupric nitrate solution (1:1 weight). After that, NaOH was added to elevate the pH of the liquid to 10. The resulting mixture was agitated overnight at 60°C , then rinsed and dried multiple times. The precipitate was then calcined for 5 h at 500°C .

2.3. Preparation of CMC/CuO-TiO₂ Nanocatalyst Beads

CuO-TiO₂ nanoparticles were dispersed in CMC solution to make CMC/CuO-TiO₂ nanocatalyst beads. Firstly, 0.1 g of CMC powder was dissolved in 50 mL of deionized water at 50 °C with stirring for 4 h. After CMC completely dissolved, 150 mg of CuO-TiO₂ nanoparticles was added to the CMC solution and continuous stirring overnight at RT (25 ± 1), which resulted in a viscous suspension. The mixture was filled in syringe and loaded by dropwise into 0.2 M AlCl₃, which used as a cross linker agent to form beads of CMC/CuO-TiO₂. The CMC/CuO-TiO₂ beads were kept in a crosslinking agent solution overnight for complete crosslinking. Afterward, the prepared beads were separated and washed several times with deionized water to eliminate the excess of unreacted Al⁺³ on the surface of the beads. Finally, the CMC/CuO-TiO₂ beads were dried at a temperature of 25 °C on the pinch top, as shown in Figure 1.

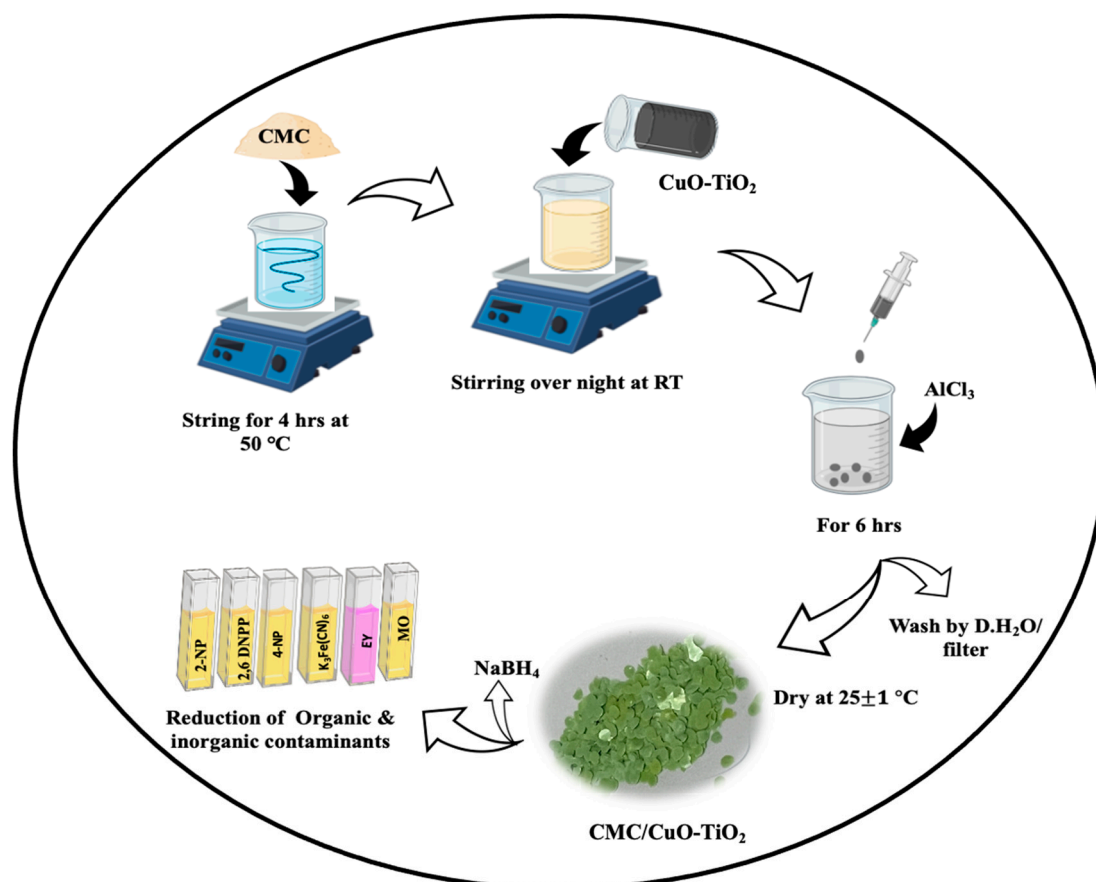


Figure 1. Schematic representation for the preparation of CMC/CuO-TiO₂ nanocatalyst beads.

2.4. Characterization

To evaluate the phase structure of the produced catalysts, X-ray diffraction (XRD) was used to confirm the morphologies and structures of CuO-TiO₂ and CMC/CuO-TiO₂. CuO-TiO₂ and CMC/CuO-TiO₂ were also analyzed using a scanning electron microscope (SEM) (JEOL, JSM-7600F, Akishima-shi, Japan) and were individually glued on the stub using carbon tape as a binder and then sputtered with platinum for 15 s. For elemental analysis, EDS was used, which is connected directly with the SEM. For UV-Vis spectra, a Thermo Scientific TM Evolution TM 350 UV-vis spectrophotometer was used to record the catalytic reduction studies.

2.5. Catalytic Reduction

The catalytic behavior of the developed nanocatalyst beads (CMC/CuO-TiO₂) was tested with organic pollutants such as nitrophenol isomers [4-NP, 2-NP, and 2,6-DNP] and

organic dyes (EY and MO) as well as inorganic compound $K_3[Fe(CN)_6]$. All these selected compounds were prepared in deionized water. In all catalytic reduction investigations, 2.5 mL of a pollutant solution was placed in the UV cuvette cell and passed across its UV-vis spectrum. After that, 0.5 mL of fresh reducing agent (0.1 M $NaBH_4$) was added, followed by 5 mg of CMC/CuO-TiO₂ beads, and the UV-vis absorption spectrum was continually recorded every 1.0 min. The percent % reduction of all compounds was calculated by utilizing Equation (1):

$$\%Reduction = \frac{C_0 - C_t}{C_0} * 100 \quad (1)$$

where C_0 and C_t are the initial and final concentrations of the studied compounds [6].

3. Result and Discussion

3.1. Characterization

3.1.1. Scanning Electron Microscope (SEM)

The surface morphology of the prepared materials CuO-TiO₂ and CMC/CuO-TiO₂ was examined using SEM. Low-to-high-magnified SEM pictures for the prepared nanocomposites are represented on the left and right sides of Figure 2. Images of Figure 2a,a' indicate the particles of CuO-TiO₂ which look like aggregated nanosheets [37,38]. The pure beads of CMC show flat surfaces with less porousness, which was presented in our previous studies [14,31]. On the other hand, CMC/CuO-TiO₂ was planted well on the CMC matrix, as observed in Figure 2b,b'. The surface of the CMC/CuO-TiO₂ beads looks smooth due to the CMC while the aggregated particles appeared due to CuO-TiO₂.

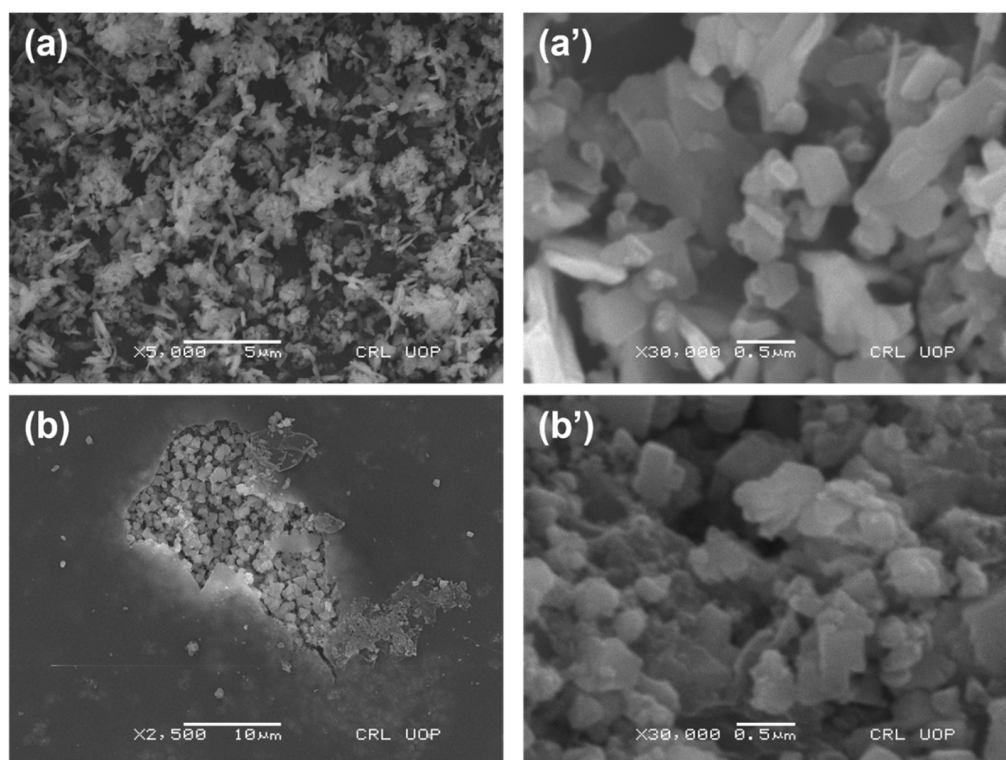


Figure 2. SEM images of (a,a') CuO-TiO₂ and (b,b') CMC/CuO-TiO₂.

3.1.2. X-ray Diffraction (XRD)

The crystal structures and phase purities of CMC/CuO-TiO₂ nanocomposite beads and CuO-TiO₂ were tested by XRD analysis. The CuO-TiO₂ nanocomposite pattern illustrated several diffraction peaks, which were indications for the CuO and TiO₂ phases. As shown in Figure 3, the diffraction peaks at 2θ were equal to 27° and 55°, confirming the TiO₂ in the rutile phase [39–41], whereas the diffraction bands at $2\theta = 35.6^\circ, 38.6^\circ,$ and 48.8° , indicating

the monoclinic structure of CuO [42]. As per our previous studies [1,38], the XRD pattern of CMC/CuO-TiO₂ bead showed one additional small hump at $2\theta = 23^\circ$ which suggest the presence of amorphous phase of CMC present in the bead. The developed CMC/CuO-TiO₂ nanocomposite beads has the same diffraction peaks, which indicating that CuO-TiO₂ was planned very well in the CMC matrix as clearly seen from Figure 3.

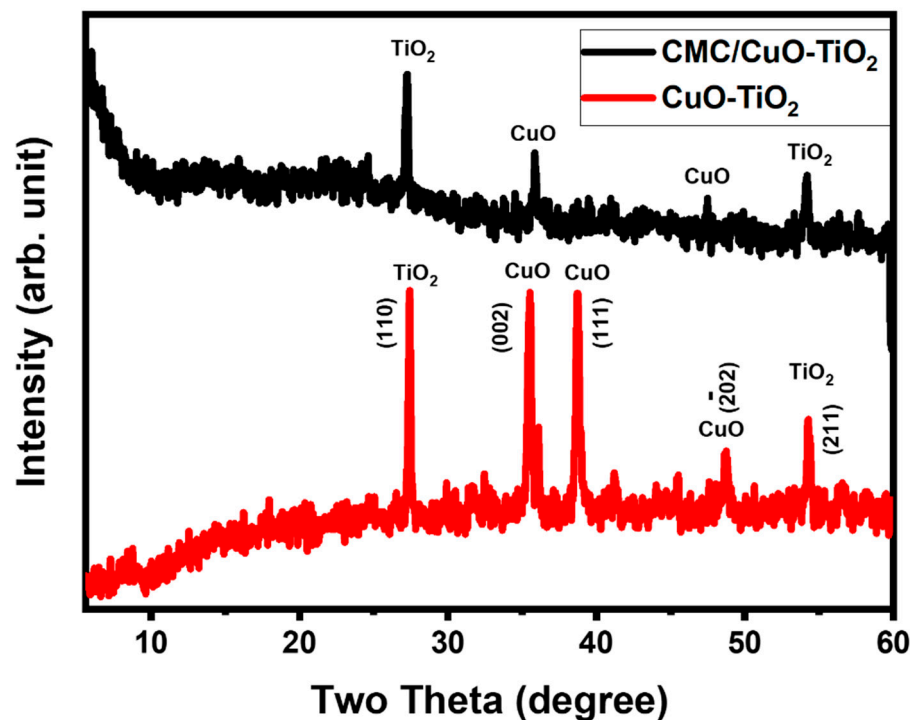


Figure 3. XRD pattern of CuO-TiO₂ and CMC/CuO-TiO₂.

3.1.3. EDS Analysis

As shown in Figure 4a,a', EDS was used to confirm the composition of CuO-TiO₂ and CMC/CuO-TiO₂ nanocatalysts. Copper (Cu), titanium (Ti), and oxygen (O) peaks were visible in the EDS spectra of the CuO-TiO₂ nanoparticles. Cu peaks were found at 0.9, 8.0, and 9.0 keV, whereas Ti peaks were found at 0.5, 4.5, and 5.0 keV, and O peaks were at 0.48 keV. Referring to Cu, Ti, and O, the data indicated the production of CuO-TiO₂ nanoparticles. Thus, the CuO-TiO₂ nanoparticles were made up of Cu, Ti, and O, according to EDS. The oxygen content was 27.32 wt% while Cu and Ti were 36.13 wt% and 33.71 wt%, according to EDS data. At the same time, the EDS analysis was also applied to CMC/CuO-TiO₂ beads. Elements such as Cu, Ti, O, C, Cl, and Al were all detected in the CMC/CuO-TiO₂ bead spectra (Figure 4b,b'), which indicated that the beads contain these elements. The production of CMC/CuO-TiO₂ beads was confirmed by these peaks. Cu, Ti, O, and C were due to CuO-TiO₂ and CMC, whereas Al and Cl were existing due to the cross-linking agent (AlCl₃). EDS proved that the developed CMC/CuO-TiO₂ beads were successfully prepared and contained Cu, Ti, O, C, Al, and Cl.

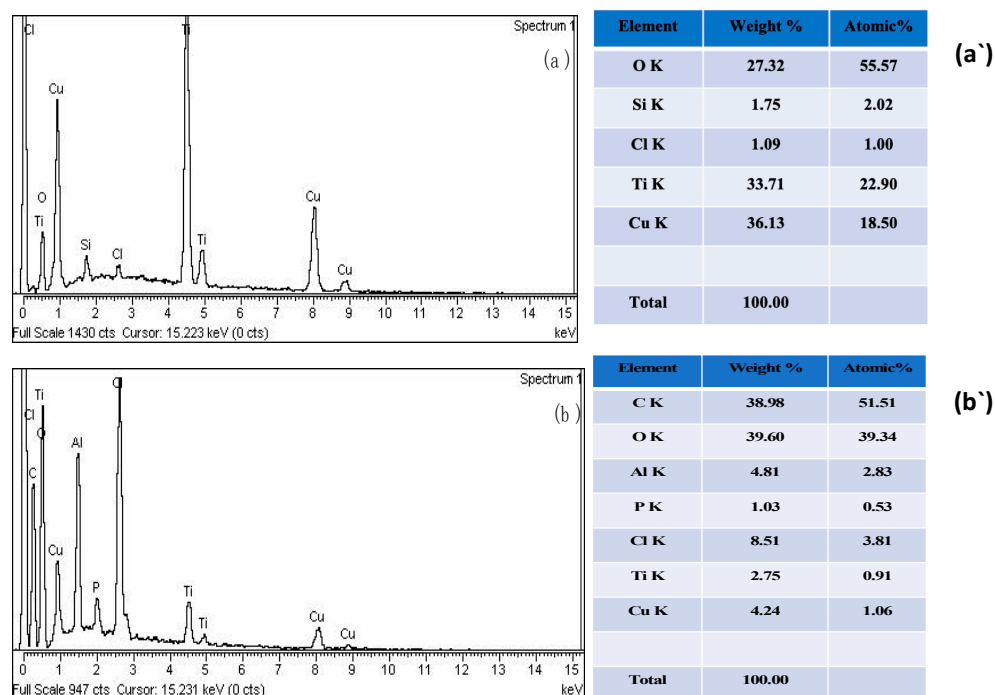


Figure 4. EDS spectrum of (a,a') CuO-TiO₂ and (b,b') CMC/CuO-TiO₂.

3.2. Catalytic Reduction

3.2.1. Reduction of Nitrophenol Isomers

The CMC/CuO-TiO₂ nanocatalyst beads were initially investigated for their ability to reduce 4-NP in the presence of NaBH₄. As can be observed in Figure 5, the 4-NP has a pale yellow absorbance peak at 317 nm. The color changed to brilliant yellow after adding 0.5 mL of 0.1 M NaBH₄, and the absorbance band was shifted to a longer wavelength of 400 nm at the same time. This is frequent in 4-NP reduction; a change in color and a shift in the absorbance band are indications of 4-nitrophenolate ion formation. However, in the absence of a catalyst, the additional conversion of 4-nitrophenolate ions to colorless amino phenol (4-AP) by NaBH₄ takes a long time, and for a few dyes, even with a large amount of reducing agent, it is not accomplished [43]. A fast and good catalytic reduction of 4-NP with only NaBH₄ would be good enough; unfortunately, it seems to be impossible to achieve it without a catalyst. Thus, a fast and good catalytic reduction of 4-NP with only NaBH₄ (without a catalyst) cannot be carried out. The excellent reduction of 4-NP requires an efficient catalyst in the presence of NaBH₄, which can speed up the reduction reaction. Therefore, CuO-TiO₂ nanocatalyst was tested for the reduction of 4-NP to 4-AP. After the introduction of CuO-TiO₂ to the mixture, the absorbance band intensity at 400 nm decreased, with the gradual disappearance of the bright yellow color. At the same time, a new absorbance band appeared at 300 nm. These results were signs of the complete reduction of the nitro group (-NO₂) in 4-NP to an amine group (-NH₂). Figure 5a shows the changes taking place during the catalytic reduction of 4-NP by CuO-TiO₂, where the reduction occurs in 12.0 min according to the spectra. However, the novel nanocatalyst beads CMC/CuO-TiO₂ were also evaluated for the catalytic reduction of 4-NP. As Figure 5a confirmed that CMC/CuO-TiO₂ performed a good catalytic reduction of 4-NP to 4-AP in a shorter period of time compared to CuO-TiO₂, where the catalytic reduction of 4-NP to 4-AP was accomplished in only 3.0 min. The fast reduction ability of CMC/CuO-TiO₂ might be due to the contribution of the Al³⁺ ion in the reduction, which had been used as a crosslinker in the preparation of beads.

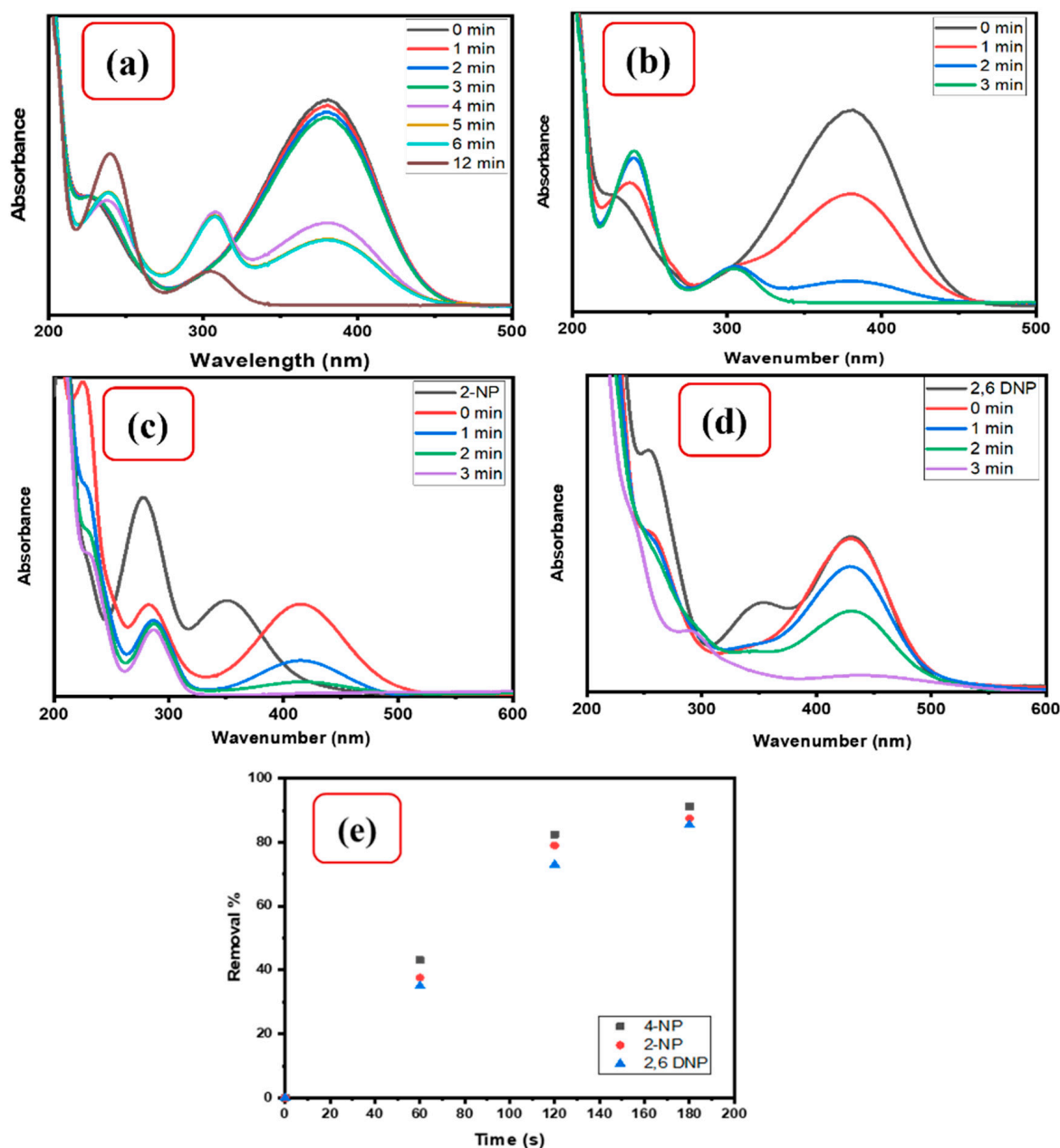


Figure 5. (a) UV-Vis spectra for 4-NP reduction using 5 mg CuO-TiO₂ in the presence of NaBH₄, (b–d), 4-NP, 2-NP, and 2,6-DNP reduction using 5 mg CMC/CuO-TiO₂ in the presence of NaBH₄, (e) removal percentage of 4-NP, 2-NP and 2,6-DNP using 5 mg CMC/CuO-TiO₂ in the presence of NaBH₄.

Similarly, under the same procedure described above, the catalytic behaviors of CMC/CuO-TiO₂ nanocatalyst beads were also tested for the catalytic reactions of nitrophenol isomers such as 2-NP and 2,6-DNP into their corresponding amino groups in the presence of 0.5 mL of 0.1 M NaBH₄. Figure 5 indicates that pure 2-NP and 2,6-DNP had strong absorbance bands at 317 nm and 428 nm, respectively. In the beginning, the catalytic reduction was examined in the absence of the nanocatalyst beads. The color of the nitrophenol isomers (2-NP and 2,6-DNP) changed from pale yellow to bright yellow, besides a slight shift of both absorption bands with only excess NaBH₄. However, using 5 mg of CMC/CuO-TiO₂ nanocatalyst beads, the 2-NP and 2,6-DNP were reduced to 2-AP and 2,6-DAP, respectively. The intensity of the absorbance peak at 413 and 428 nm steadily dropped as the process progressed, while a new absorbance band developed at

280 nm with increased intensity (Figure 5c,d). The spectra revealed that the reduction reaction of 2-NP and 2,6-DNP occurred within 3.0 min. The removal percentage of the reduction process was estimated using Equation (1). The reduction of nitrophenol isomers 4-NP, 2-NP, and 2,6-DNP were found to be 90.24%, 87.5%, and 85.43%, respectively. The CMC/CuO-TiO₂ nanocatalyst was efficient, selective, and had excellent catalytic activity toward nitrophenol isomers.

Figure 6 depicts the schematic representation of 4-NP reduction mechanism. In accordance with this scheme, it is proposed that initially both BH₄⁻ and 4-NP get adsorbed on the surface of the catalyst. The catalyst enhances the transfer of electron from BH₄⁻ to 4-NP and thus decreases the activation energy of the reaction.

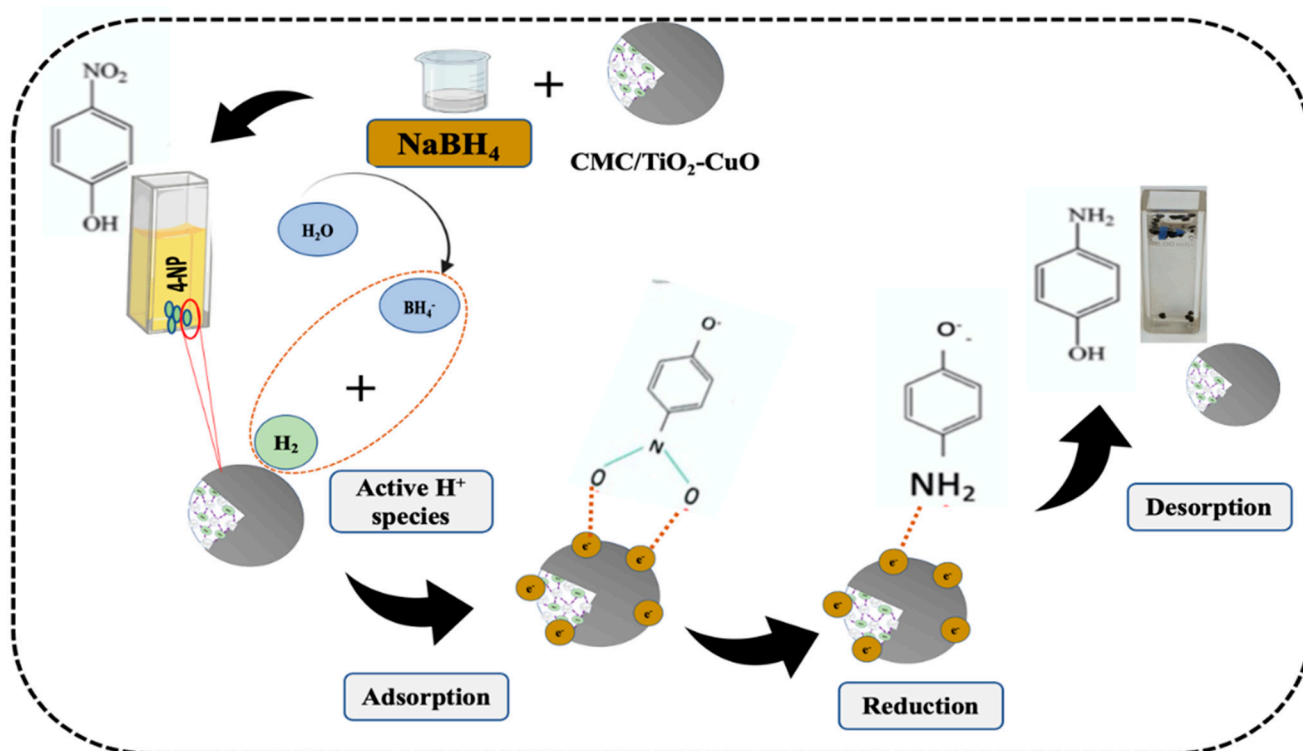


Figure 6. Schematic representation for the catalytic reduction of 4-NP.

Effect of 4-Nitrophenol Concentration

The effect of 4-NP concentration on the catalytic activity of CMC/CuO-TiO₂ was studied using 0.1 M NaBH₄. For this investigation, three different concentrations of 4-NP solution (0.13, 0.08, and 0.04 mM) were prepared to determine the catalytic effects of 4-NP concentration. Figure 7 indicated the spectra of a range of 4-NP concentrations, in which 0.13 mM concentration reduced up to 90% in 3.0 min and up to 83% and 80% in 2.0 and 1.30 min for 0.08 and 0.04 mM, respectively. As a result, it was noticed that as compared to higher concentrations of 4-NP, the low concentration could be easily reduced while the catalyst quantity remained constant [1].

Effect of NaBH₄ Concentration

The influence of NaBH₄ concentration on the catalytic reduction of 4-NP was studied by using CMC/CuO-TiO₂ nanocatalyst beads. Various doses of NaBH₄ (0.1 M and 0.05 M) were employed in the presence of 5 mg CMC/CuO-TiO₂ beads in this work. Based on the results, increasing the NaBH₄ concentration led to speeding up the reaction, as shown in the UV-Vis spectra of the catalytic reduction of 4-NP in Figure 8. With 0.1 M and 0.05 M, 4-NP was reduced up to 90% and 92%, respectively. As a result, it was shown that 0.1 M NaBH₄ concentration could speed up the reaction and reduce the 4-NP in less time than 0.05 M concentration of NaBH₄.

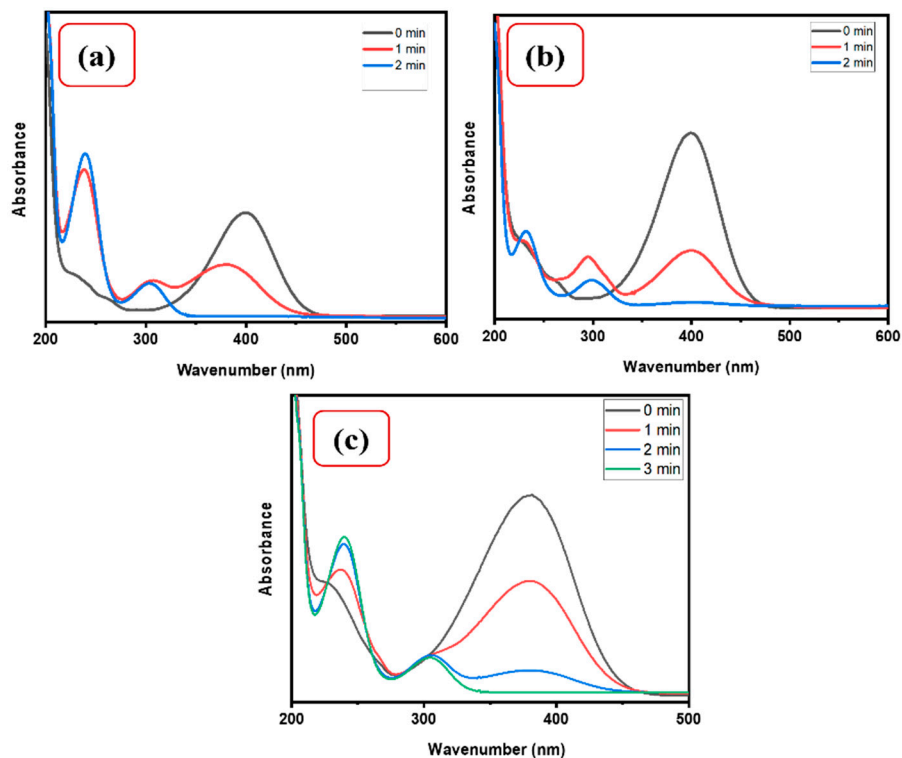


Figure 7. UV-Vis spectra for (a) 0.04, (b) 0.08, and (c) 0.13 mM 4-NP using 5 mg CMC/CuO-TiO₂ in the presence of NaBH₄.

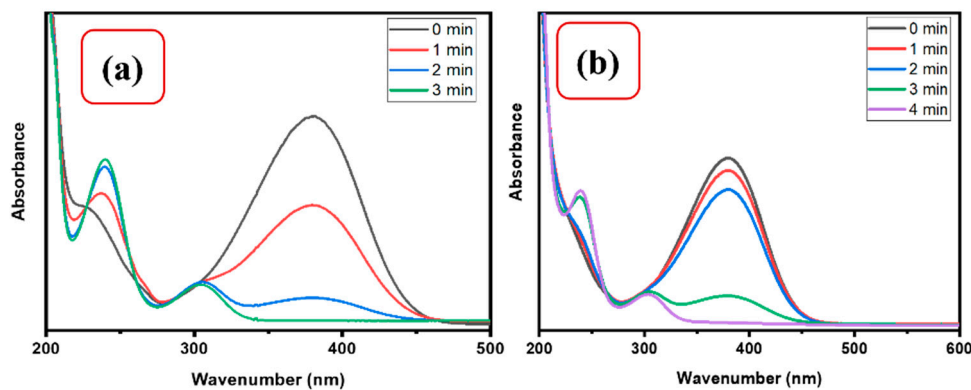


Figure 8. UV-Vis spectra for 0.13 mM 4-NP in the presence of (a) 0.5 M and (b) 0.1 M NaBH₄ using 5 mg CMC/CuO-TiO₂.

3.2.2. Reduction of Organic Dyes

Organic dyes are widely used in the textile industry, and their non-biodegradability, toxicity, mutagenicity, and carcinogenicity make them a growing source of pollution in the environment. The goal of this investigation was to see how well the newly designed nanocatalyst beads reduce two types of organic dyes: methyl orange (MO) and eosin yellow (EY). UV-Vis spectroscopy was used to record the catalytic reduction, as shown in Figure 9a,b.

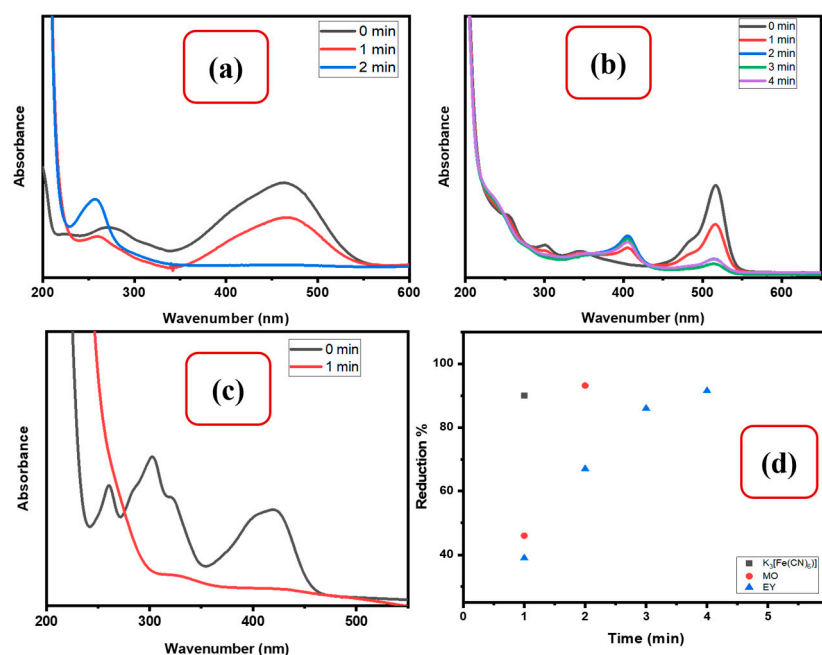


Figure 9. UV-Vis spectra for catalytic reduction of (a) MO, (b) EY, and (c) K₃[Fe(CN)₆] using CMC/CuO-TiO₂ beads in the presence of NaBH₄, (d) removal percentage of MO, EY, and K₃[Fe(CN)₆] using 5 mg CMC/CuO-TiO₂ in the presence of NaBH₄.

The catalytic reduction of MO and EY was tested using 5 mg of CMC/CuO-TiO₂ nanocatalyst beads in the presence of NaBH₄. In the addition of only NaBH₄, no reductive reaction could take place between NaBH₄ and the dyes. However, a regular decrease in the adsorption band was observed in the presence of CMC/CuO-TiO₂ nanocatalyst beads. The catalytic reduction was recorded via UV-Vis spectroscopy. As clearly seen from (Figure 9a,b), the removal (%) of EY and MO occurred within 1.0–4.0 min, which reduced MO and EY up to 93.14%, and 91.5%, respectively (Figure 9d). Electrons were transferred from BH₄[−] to CMC/CuO-TiO₂ and then to acceptor dye molecules, reducing the azo (-N=N-) group found in dye molecules, according to recent results [1].

3.2.3. Reduction of Inorganic Complex

Inorganic contaminants such as K₃[Fe(CN)₆] are known as pollutants that are distributed in the environment in either soil or water. Accordingly, K₃[Fe(CN)₆] can cause acute toxicity and carcinogenicity at very low levels, and it has been proven to easily accumulate inside human beings via food chains [44,45]. Due to this, K₃[Fe(CN)₆] was chosen as one of our selected pollutants. To test the catalytic activity of CMC/CuO-TiO₂ beads, they were used to catalyze the reduction of K₃[Fe(CN)₆]. The UV-Vis absorbance of the catalytic reduction of K₃[Fe(CN)₆] was monitored to check the progress of the K₃[Fe(CN)₆] reaction. Using CMC/CuO-TiO₂, the absorption band of K₃[Fe(CN)₆] at 420 nm was gradually lowered in 1.0 min, with the yellow color disappearing, indicating the complete reduction of K₃[Fe(CN)₆] to K₄[Fe(CN)₆] [44]. Figure 9c shows the transformation of 90% of K₃[Fe(CN)₆] to K₄[Fe(CN)₆], which was obtained in only 1.0 min.

An electron-transfer reaction is the probable mechanism for the reaction of K₃[Fe(CN)₆] in the presence of catalyst beads and NaBH₄, as indicated in Equation (2) below [1,44].



As a result, there are two steps in the catalytic reaction mechanism of K₃[Fe(CN)₆]. The reducing agent NaBH₄ causes the polarization of the catalyst nanocomposite beads at first. Subsequently, electrons are transported from the catalyst surface to the [Fe(CN)₆]^{−3}

pollutant, where they are reduced to $[\text{Fe}(\text{CN})_6]^{-4}$. The obtained reduction results of all studied compounds were compared with the literature, as shown in Table 1 [1,6,18,27,42,46–48].

Table 1. Comparison of the catalytic reduction of 4-NP, MO, EY, and $\text{K}_3[\text{Fe}(\text{CN})_6]$ by using CMC/CuO-TiO₂ beads in the presence of NaBH₄ with other reported catalysts.

Pollutant	Catalyst	Time (s)	Reference
4-NP	CMC/CuO-TiO ₂	180	This Work
4-NP	Co-Cu/CIN/SCMC/TiO ₂	240	[27]
4-NP	<i>cf</i> -CA-AuNPs	900	[46]
4-NP	Fe ₃ O ₄ /TiO ₂ /CuO	120	[18]
MO	CMC/CuO-TiO ₂	120	This Work
MO	CA-ZA10@Ni NPs	1080	[47]
MO	Ni/Cs@CMC/CuO-Co ₂ O ₃	120	[42]
EY	CMC/CuO-TiO ₂	240	This Work
EY	Ni/Cs@CMC/CuO-Co ₂ O ₃	360	[42]
EY	MnFe ₂ O ₄ @PANI@Ag	420	[48]
$\text{K}_3[\text{Fe}(\text{CN})_6]$	CMC/CuO-TiO ₂	60	This Work
$\text{K}_3[\text{Fe}(\text{CN})_6]$	Ni/Cs@CMC/CuO-Co ₂ O ₃	360	[42]
$\text{K}_3[\text{Fe}(\text{CN})_6]$	Alg@Cu ₂ O-Sb ₂ O ₃	180	[6]
$\text{K}_3[\text{Fe}(\text{CN})_6]$	CMC/CuO-NiO	40	[1]

3.2.4. Catalyst Stability and Reusability

Besides the activity of catalysts, stability is also a critical factor for evaluating their efficiency and potential applications. For this study, the stability of CMC/CuO-TiO₂ nanocatalyst beads was examined regarding the catalytic reduction of 4-NP, and we found that the beads were stable for up to more than one year without any degradation or loss of activity. The recyclability of CMC/CuO-TiO₂ beads was also studied for the catalytic reduction of 4-NP under the same conditions described in the experimental part. The CMC/CuO-TiO₂ nanocatalyst beads were examined over four cycles, and the beads were washed three times after each use with distilled water and dried at RT. The catalytic reduction of 4-NP took 3.0 min for the first use, and 4.0 min, 6.0 min, and 11.0 min for the second, third, and fourth cycles, respectively (Figure 10). This suggests that the catalyst was active and effective in the reduction of 4-NP. Thus, the CMC/CuO-TiO₂ beads were able to be used up to four cycles.

3.2.5. Catalytic Efficiency of CMC/CuO-TiO₂ Beads in Real Samples

To evaluate the efficiency of the CMC/CuO-TiO₂ nanocatalyst beads under optimized conditions, four types of real samples were used (orange juice, full-fat milk, seawater, and wastewater), which were collected or obtained from a local market (Jeddah, Saudi Arabia). Real samples were prepared by diluting approximately 1 mL of each sample in 100 mL of deionized water individually. Afterwards, 2.5 mL of each sample was then transferred into a cuvette cell, together with 0.5 mL of 0.13 mM 4-NP, 0.5 mL of 0.1 M NaBH₄, and 5 mg of CMC/CuO-TiO₂ nanocatalyst beads. A UV-Vis spectrophotometer was used to monitor the catalytic reduction of 4-NP. As can be observed from the data in Table 2, full-fat milk and seawater have low reduction percentages, which reduced by up to 79.4% in 10.0 min and 82.5% in 11.0 min, respectively. This is because there was a lot of interference in these samples, which can impact the catalytic reduction of 4-NP. The reduction of 4-NP in the other samples took 5.0 min and was 92–89%. The results showed that the CMC/CuO-TiO₂ nanocatalyst was effective in decolorizing and reducing of 4-NP from the real samples.

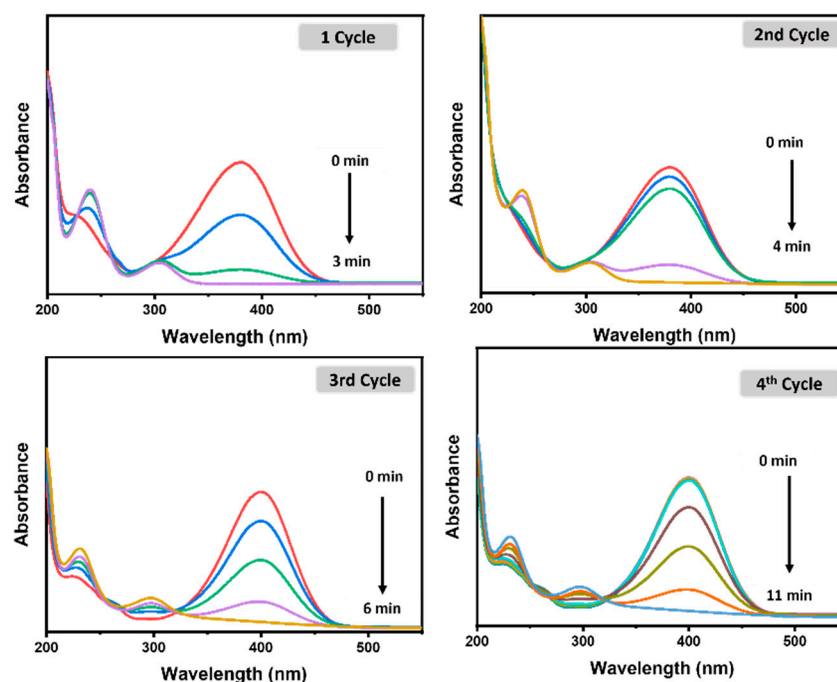


Figure 10. UV-Vis spectra for recyclability of CMC/CuO-TiO₂ beads toward the catalytic reduction of 0.13 mM 4-NP.

Table 2. Application of CMC/CuO-TiO₂ nanocatalyst beads on four types of real samples spiked with 4-NP.

Real Sample	Reduction Time (min)	% Reduction
Orange Juice	5.0	92.6%
Full-Fat Milk	10.0	79.4%
Wastewater	5.0	89.2
Seawater	11.0	82.5%

4. Conclusions

Herein, a simple and potentially cost-effective method was used for the fabrication of nanocatalyst CMC/CuO-TiO₂ beads. The CMC/CuO-TiO₂ beads were analyzed using SEM, XRD and EDS. The developed beads exhibited high catalytic activity toward nitrophenol isomers (4-NP, 2-NP, and 2,6-DNP), organic dyes (MO and EY), and inorganic complex K₃[Fe(CN)₆]. The developed materials can act as promising nanocatalysts for water treatment purposes.

Author Contributions: Conceptualization, S.B.K.; methodology, N.M.; software, K.A.; validation, K.A. and A.M.A.; formal analysis, E.Y.D. and K.A.; investigation, E.M.B. and N.M.; resources, A.M.A.; data curation, E.M.B.; writing—original draft preparation, N.M.; writing—review and editing, E.M.B., S.B.K., E.Y.D. and K.A.; supervision, E.Y.D. and A.M.A.; funding acquisition, E.M.B. All authors have read and agreed to the published version of the manuscript.

Funding: This project was funded by the Deanship of Scientific Research (DSR) at King Abdulaziz University, Jeddah, Saudi Arabia under grant no. (G: 54-247-1441).

Institutional Review Board Statement: Not applicable.

Informed Consent Statement: Not applicable.

Data Availability Statement: The data presented in this study are available on request from the corresponding author.

Acknowledgments: This project was funded by the Deanship of Scientific Research (DSR) at King Abdulaziz University, Jeddah, Saudi Arabia under grant no. (G: 54-247-1441). The authors, therefore, acknowledge with thanks DSR for technical and financial support.

Conflicts of Interest: The authors declare no conflict of interest.

References

1. Maslamani, N.; Khan, S.B.; Danish, E.Y.; Bakhsh, E.M.; Zakeeruddin, S.M.; Asiri, A.M. Carboxymethyl cellulose nanocomposite beads as super-efficient catalyst for the reduction of organic and inorganic pollutants. *Int. J. Biol. Macromol.* **2021**, *167*, 101–116. [[CrossRef](#)] [[PubMed](#)]
2. Sohni, S.; Norulaini, N.N.; Hashim, R.; Khan, S.B.; Fadhillah, W.; Omar, A.M. Physicochemical characterization of Malaysian crop and agro-industrial biomass residues as renewable energy resources. *Ind. Crop. Prod.* **2018**, *111*, 642–650. [[CrossRef](#)]
3. Ismail, M.; Gul, S.; Khan, M.; Asiri, A.M.; Khan, S.B. Green synthesis of zerovalent copper nanoparticles for efficient reduction of toxic azo dyes congo red and methyl orange. *Green Process. Synth.* **2019**, *8*, 135–143. [[CrossRef](#)]
4. Khan, S.A.; Khan, S.B.; Asiri, A.M. Layered double hydroxide of Cd-Al/C for the mineralization and de-coloration of dyes in solar and visible light exposure. *Sci. Rep.* **2016**, *6*, 35107. [[CrossRef](#)] [[PubMed](#)]
5. Jang, E.S.; Khan, S.B.; Seo, J.; Akhtar, K.; Choi, J.; Kim, K.I.; Han, H. Synthesis and characterization of novel UV-curable PU-Si hybrids: Influence of silica on thermal, mechanical, and water sorption properties of polyurethane acrylates. *Macromol. Res.* **2011**, *19*, 1006–1013. [[CrossRef](#)]
6. Khan, S.B.; Bakhsh, E.M.; Akhtar, K.; Kamal, T.; Shen, Y.; Asiri, A.M. Copper oxide-antimony oxide entrapped alginate hydrogel as efficient catalyst for selective reduction of 2-nitrophenol. *Polymers* **2022**, *14*, 458. [[CrossRef](#)]
7. Maslamani, N.; Manandhar, E.; Geremia, D.K.; Logue, B.A. ICE concentration linked with extractive stirrer (ICECLES). *Anal. Chim. Acta* **2016**, *941*, 41–48. [[CrossRef](#)] [[PubMed](#)]
8. Kim, D.; Jung, J.; Kim, Y.; Lee, M.; Seo, J.; Khan, S.B. Structure and thermal properties of octadecane/expanded graphite composites as shape-stabilized phase change materials. *Int. J. Heat Mass Transf.* **2016**, *95*, 735–741. [[CrossRef](#)]
9. Zhang, P.; Sui, Y.; Xiao, G.; Wang, Y.; Wang, C.; Liu, B.; Zou, G.; Zou, B. Facile fabrication of faceted copper nanocrystals with high catalytic activity for p-nitrophenol reduction. *J. Mater. Chem. A* **2013**, *1*, 1632–1638. [[CrossRef](#)]
10. Farooqi, Z.H.; Sakhawat, T.; Khan, S.R.; Kanwal, F.; Usman, M.; Begum, R. Synthesis, characterization and fabrication of copper nanoparticles in N-isopropylacrylamide based co-polymer microgels for degradation of p-nitrophenol. *Mater. Sci.* **2015**, *33*, 185–192. [[CrossRef](#)]
11. Benhadria, N.; Hachemaoui, M.; Zaoui, F.; Mokhtar, A.; Boukreris, S.; Attar, T.; Belarbi, L.; Boukoussa, B. Catalytic reduction of methylene blue dye by copper oxide nanoparticles. *J. Clust. Sci.* **2022**, *33*, 249–260. [[CrossRef](#)]
12. Ren, Z.-H.; Li, H.-T.; Gao, Q.; Wang, H.; Han, B.; Xia, K.-S.; Zhou, C.-G. Au nanoparticles embedded on urchin-like TiO₂ nanosphere: An efficient catalyst for dyes degradation and 4-nitrophenol reduction. *Mater. Des.* **2017**, *121*, 167–175. [[CrossRef](#)]
13. Guo, X.; Chen, F. Removal of arsenic by bead cellulose loaded with iron oxyhydroxide from groundwater. *Environ. Sci. Technol.* **2005**, *39*, 6808–6818. [[CrossRef](#)]
14. Sundaram, M.; Kalpana, S.; Sivaganesan, V.; Nandhakumar, E. Studies on the catalytic activity of CuO/TiO₂/ZnO ternary nanocomposites prepared via one step hydrothermal green approach. *Mater. Res. Express* **2019**, *6*, 125043.
15. Li, P.; Zhang, X.; Wang, J.; Xu, B.; Zhang, X.; Fan, G.; Zhou, L.; Liu, X.; Zhang, K.; Jiang, W. Binary CuO/TiO₂ nanocomposites as high-performance catalysts for tandem hydrogenation of nitroaromatics. *Colloids Surfaces A Physicochem. Eng. Asp.* **2021**, *629*, 127383. [[CrossRef](#)]
16. Bakre, P.V.; Kamat, D.P.; Mandrekar, K.S.; Tilve, S.G.; Ghosh, N.N. CuO-NiO-TiO₂ bimetallic nanocomposites for catalytic applications. *Mol. Catal.* **2020**, *496*, 111193. [[CrossRef](#)]
17. Akbari, R. Green synthesis and catalytic activity of copper nanoparticles supported on TiO₂ as a highly active and recyclable catalyst for the reduction of nitro-compounds and degradation of organic dyes. *J. Mater. Sci. Mater. Electron.* **2021**, *32*, 15801–15813. [[CrossRef](#)]
18. Kianfar, A.H.; Arayesh, M.A. Synthesis, characterization and investigation of photocatalytic and catalytic applications of Fe₃O₄/TiO₂/CuO nanoparticles for degradation of MB and reduction of nitrophenols. *J. Environ. Chem. Eng.* **2020**, *8*, 103640. [[CrossRef](#)]
19. Bathla, A.; Rather, R.A.; Poonia, T.; Pal, B. Morphology dependent photocatalytic activity of CuO/CuO-TiO₂ nanocatalyst for degradation of methyl orange under sunlight. *J. Nanosci. Nanotechnol.* **2020**, *20*, 3123–3130. [[CrossRef](#)] [[PubMed](#)]
20. Gupta, S.; Pathak, A.K.; Ameta, C.; Punjabi, P.B. Microwave-induced expeditious synthesis of biologically active substituted imidazoles using CuO-TiO₂-GO nanocomposite as a recyclable catalyst. *Lett. Org. Chem.* **2021**, *18*, 318–333. [[CrossRef](#)]
21. Lee, Y.; Kim, D.; Seo, J.; Han, H.; Khan, S.B. Preparation and characterization of poly(propylene carbonate)/exfoliated graphite nanocomposite films with improved thermal stability, mechanical properties and barrier properties. *Polym. Int.* **2013**, *62*, 1386–1394. [[CrossRef](#)]
22. Ismail, M.; Khan, M.; Akhtar, K.; Asiri, A.M.; Khan, S.B. Biosynthesis of silver nanoparticles: A colorimetric optical sensor for detection of hexavalent chromium and ammonia in aqueous solution. *Phys. E Low Dimens. Syst. Nanostruct.* **2018**, *103*, 367–376. [[CrossRef](#)]

23. Khan, S.B.; Khan, S.A.; Asiri, A.M. A fascinating combination of Co, Ni and Al nanomaterial for oxygen evolution reaction. *Appl. Surf. Sci.* **2016**, *370*, 445–451. [[CrossRef](#)]
24. Sikora, E.; Katona, K.K.; Muránszky, G.; Bánhidi, O.; Kristály, F.; Szabó, J.T.; Windisch, M.; Fiser, B.; Vanyorek, L. Cellulose-based catalyst design for efficient chlorate reduction. *Arab. J. Chem.* **2021**, *14*, 103202. [[CrossRef](#)]
25. Anwar, Y.; Ali, H.S.M.; Rehman, W.U.; Hemeg, H.A.; Khan, S.A. Antibacterial films of alginate-CoNi-coated cellulose paper stabilized Co NPs for dyes and nitrophenol degradation. *Polymers* **2021**, *13*, 4122. [[CrossRef](#)] [[PubMed](#)]
26. El Sayed, A.M.; Saber, S. Structural, optical analysis, and Poole–Frenkel emission in NiO/CMC–PVP: Bio-nanocomposites for optoelectronic applications. *J. Phys. Chem. Solids* **2022**, *163*, 110590. [[CrossRef](#)]
27. Althomali, R.H.; Alamry, K.A.; Hussein, M.A.; Khan, A.; Alosaimi, A.M. A green nanocomposite based modified cellulose/TiO₂/cinnamon bark for the reduction of toxic organic compounds using spectrophotometric technique. *J. Mater. Res. Technol.* **2021**, *12*, 947–966. [[CrossRef](#)]
28. Kamal, T.; Ahmad, I.; Khan, S.B.; Asiri, A.M. Bacterial cellulose as support for biopolymer stabilized catalytic cobalt nanoparticles. *Int. J. Biol. Macromol.* **2019**, *135*, 1162–1170. [[CrossRef](#)]
29. Khan, M.S.J.; Khan, S.B.; Kamal, T.; Asiri, A.M. Agarose biopolymer coating on polyurethane sponge as host for catalytic silver metal nanoparticles. *Polym. Test.* **2019**, *78*, 105983. [[CrossRef](#)]
30. Bakhsh, E.M.; Akhtar, K.; Fagieh, T.M.; Khan, S.B.; Asiri, A.M. Development of alginate@tin oxide–cobalt oxide nanocomposite based catalyst for the treatment of wastewater. *Int. J. Biol. Macromol.* **2021**, *187*, 386–398. [[CrossRef](#)]
31. Maslamani, N.; Khan, S.B.; Danish, E.Y.; Bakhsh, E.M.; Akhtar, K.; Asiri, A.M. Metal nanoparticles supported chitosan coated carboxymethyl cellulose beads as a catalyst for the selective removal of 4-nitrophenol. *Chemosphere* **2022**, *291*, 133010. [[CrossRef](#)]
32. Jang, E.S.; Khan, S.B.; Seo, J.; Nam, Y.H.; Choi, W.J.; Akhtar, K.; Han, H. Synthesis and characterization of novel UV-curable polyurethane–clay nanohybrid: Influence of organically modified layered silicates on the properties of polyurethane. *Prog. Org. Coat.* **2011**, *71*, 36–42. [[CrossRef](#)]
33. Khan, S.B.; Rahman, M.M.; Jang, E.S.; Akhtar, K.; Han, H. Special susceptible aqueous ammonia chemi-sensor: Extended applications of novel UV-curable polyurethane–clay nanohybrid. *Talanta* **2011**, *84*, 1005–1010. [[CrossRef](#)] [[PubMed](#)]
34. Khan, S.A.; Khan, S.B.; Asiri, A.M. Toward the design of Zn–Al and Zn–Cr LDH wrapped in activated carbon for the solar assisted de-coloration of organic dyes. *RSC Adv.* **2016**, *6*, 83196–83208. [[CrossRef](#)]
35. Kamal, T.; Ali, N.; Naseem, A.A.; Khan, S.B.; Asiri, A.M. Polymer nanocomposite membranes for antifouling nanofiltration. *Recent Pat. Nanotechnol.* **2016**, *10*, 189–201. [[CrossRef](#)] [[PubMed](#)]
36. Tahseen, K.; Ikram, A.; Khan, S.B.; Asiri, A.M. Agar hydrogel supported metal nanoparticles catalyst for pollutants degradation in water. *Desalin. Water Treat.* **2018**, *136*, 290–298.
37. Rokhmat, M.; Wibowo, E.; Abdullah, M. Performance improvement of TiO₂/CuO solar cell by growing copper particle using fix current electroplating method. *Procedia Eng.* **2017**, *170*, 72–77. [[CrossRef](#)]
38. Liu, L.; Gu, X.; Sun, C.; Li, H.; Deng, Y.; Gao, F.; Dong, L. In situ loading of ultra-small Cu₂O particles on TiO₂ nanosheets to enhance the visible-light photoactivity. *Nanoscale* **2012**, *4*, 6351–6359. [[CrossRef](#)] [[PubMed](#)]
39. Abdel-Galil, A.; Ali, H.; Atta, A.; Balboul, M. Influence of nanostructured TiO₂ additives on some physical characteristics of carboxymethyl cellulose (CMC). *J. Radiat. Res. Appl. Sci.* **2014**, *7*, 36–43. [[CrossRef](#)]
40. Ali, H.; Atta, A.; Senna, M. Physico-chemical properties of carboxymethyl cellulose (CMC)/nanosized titanium oxide (TiO₂) gamma irradiated composite. *Arab. J. Nucl. Sci. Appl.* **2015**, *48*, 44–52.
41. Shoukat, A.; Wahid, F.; Khan, T.; Siddique, M.; Nasreen, S.; Yang, G.; Ullah, M.W.; Khan, R. Titanium oxide-bacterial cellulose bioadsorbent for the removal of lead ions from aqueous solution. *Int. J. Biol. Macromol.* **2019**, *129*, 965–971. [[CrossRef](#)]
42. Maslamani, N.; Bakhsh, E.M.; Khan, S.B.; Danish, E.Y.; Akhtar, K.; Fagieh, T.M.; Su, X.; Asiri, A.M. Chitosan@carboxymethylcellulose/CuO–CO₂O₃ nanoadsorbent as a super catalyst for the removal of water pollutants. *Gels* **2022**, *8*, 91. [[CrossRef](#)]
43. Ahmad, I.; Kamal, T.; Khan, S.B.; Asiri, A.M. An efficient and easily retrievable dip catalyst based on silver nanoparticles/chitosan-coated cellulose filter paper. *Cellulose* **2016**, *23*, 3577–3588. [[CrossRef](#)]
44. Veerakumar, P.; Salamalai, K.; Thanasekaran, P.; Lin, K.-C. Simple preparation of porous carbon-supported ruthenium: Propitious catalytic activity in the reduction of ferrocyanate(III) and a cationic dye. *ACS Omega* **2018**, *3*, 12609–12621. [[CrossRef](#)] [[PubMed](#)]
45. Xia, Q.; Fu, S.; Ren, G.; Chai, F.; Jiang, J.; Qu, F. Fabrication of Fe₃O₄@Au hollow spheres with recyclable and efficient catalytic properties. *New J. Chem.* **2016**, *40*, 818–824. [[CrossRef](#)]
46. Seo, Y.S.; Ahn, E.-Y.; Park, J.; Kim, T.Y.; Hong, J.E.; Kim, K.; Park, Y.; Park, Y. Catalytic reduction of 4-nitrophenol with gold nanoparticles synthesized by caffeic acid. *Nanoscale Res. Lett.* **2017**, *12*, 7. [[CrossRef](#)] [[PubMed](#)]
47. Khan, S.A.; Bakhsh, E.M.; Akhtar, K.; Khan, S.B. A template of cellulose acetate polymer–ZnAl/C layered double hydroxide composite fabricated with Ni NPs: Applications in the hydrogenation of nitrophenols and dyes degradation. *Spectrochim. Acta Part A Mol. Biomol. Spectrosc.* **2020**, *241*, 118671. [[CrossRef](#)] [[PubMed](#)]
48. Amir, M.; Kurtan, U.; Baykal, A.; Sözeri, H. MnFe₂O₄@PANI@Ag heterogeneous nanocatalyst for degradation of industrial aqueous organic pollutants. *J. Mater. Sci. Technol.* **2016**, *32*, 134–141. [[CrossRef](#)]

Disclaimer/Publisher’s Note: The statements, opinions and data contained in all publications are solely those of the individual author(s) and contributor(s) and not of MDPI and/or the editor(s). MDPI and/or the editor(s) disclaim responsibility for any injury to people or property resulting from any ideas, methods, instructions or products referred to in the content.